Shot noise suppression in $p - n$ junctions due to carrier generation-recombination

I. A. Maione,[1,2] B. Pellegrini,[1] G. Fiori,[1] M. Macucci,[1] L. Guidi,[1] and G. Basso[1]

[1]*Dipartimento di Ingegneria dell'Informazione: Elettronica, Informatica, Telecomunicazioni, Università di Pisa, Via Caruso 16, I-56122, Pisa, Italy*

[2]*Karlsruher Institut für Technologie (KIT), Institut für Neutronenphysik und Reaktortechnik, Hermann-von-Helmholtz-Platz 1, D-76344 Eggenstein-Leopoldshafen, Germany*

(Received 24 November 2010; published 15 April 2011)

We present a theoretical and experimental investigation of shot noise suppression in gallium arsenide and silicon $p - n$ junctions due the to effect of generation-recombination phenomena. In particular, the availability of the cross-correlation technique and of ultra-low-noise amplifiers has allowed us to significantly extend, down to 10 pA, the range of bias current values for which results were available in the literature. To provide a quantitative understanding of the observed V-shape noise behavior, we have extended the Shockley-Read-Hall model for the trap-assisted generation-recombination mechanism. Such a model has represented the theoretical background for the performed Monte Carlo noise simulations, which have provided good agreement with the experimental results.

DOI: 10.1103/PhysRevB.83.155309 PACS number(s): 72.20.Jv, 07.50.Hp, 72.70.+m

I. INTRODUCTION

Suppression of shot noise below the level predicted by Schottky's theorem[1] ($S_I = 2qI$, where q is the electronic charge and I is the average current) as a result of correlations of different nature among charge carriers has been attracting significant interest in condensed matter physics because it represents a link between an easily accessible macroscopic quantity, the shot noise power spectral density, and microscopic properties of devices and materials.

The extensive review by Blanter and Büttiker[2] provides a detailed overview of the field, discussing the different interactions that may lead to correlations between charge-carrier traversal events in mesoscopic devices. One of the early studied shot noise suppression effects in nanostructures is that observed in double-barrier resonant tunneling devices (DBRTDs), where, in the positive differential resistance region, a Fano factor (ratio of the noise power spectral density to that predicted by Schottky's theorem) down to 1/2 was observed by Li *et al.*,[3] and which is due to an interplay between Pauli and Coulomb correlations.[4–7] In the negative differential resistance region, instead, a shot noise enhancement was observed[8] due to positive correlations among charge carriers resulting from the quantum well electrostatics.

Shot noise suppression does not occur only in low-dimensional structures, but also in $p - n$ junctions when a large contribution to the current comes from charge generation-recombination (g-r) in the depletion region, as demonstrated theoretically[9–11] and experimentally[12,13] since a long time ago. As in the shot noise suppression in double-barrier resonant tunneling devices, correlation between carriers is introduced by the fact that there are states (trap states in this case, well states in DBRTDs), the occupancy of which regulates the carrier flux. While in DBRTDs there is, as mentioned above, a subtle interplay between Pauli and Coulomb exclusion, in the $p - n$ junction, unless the trap density is very large, the carrier correlation is mainly due just to Pauli exclusion.

Initial experimental results by Schneider and Strutt[12] did not provide clear evidence of a suppression in $p - n$ junctions, which was also due to the insufficient sensitivity of the measurement equipment available at the time. Wade and van der Ziel,[13] instead, operated at low temperature (at 100 K) where the g-r component is larger than at room temperature, observing a clear noise suppression (down to a factor of about 0.8). In their results, the Fano factor increases with increasing current (within the measurement interval), reaching a value of about 0.87 at 1.5 mA. The theoretical models existing at the time, or developed shortly thereafter, did not explain this dependence of noise on current and, indeed, the authors of Ref. 13 as well as van Vliet (who developed a more advanced model[10] leading to results similar those of Lauritzen[9]) conclude that a revised theory is needed to explain the experimental data. Blasquez[14] obtained some further experimental results, limited to a narrow current interval and affected by a large dispersion, that he interpreted as consistent with the existing theories. Dai and Chen[15] claimed a noise level much higher than full shot, but they had a quadratic dependence on current; therefore, they were not observing shot noise but classical generation-recombination noise associated with carrier number fluctuations.

There was actually no other theoretical work on the subject until 2001, when Jimenez Tejada *et al.*,[11] on the basis of the response of an electric field to fluctuations of the trapped charge, obtained a model predicting full shot noise at low bias currents and, as the current is increased, a decrease of the Fano factor, followed by a very abrupt increase that leads to values beyond 2. This last effect is not clearly justified on intuitive grounds and has not been observed experimentally.

This is the reason why we have focused on noise measurements performed at room temperature on three different types of $p - n$ junctions, using a cross-correlation technique that has allowed us to investigate noise levels well below those of the papers from the 1970s and to operate over a much wider current interval, up to four current decades, starting from 10 pA.[16]

We have focused our attention on a GaAs diode and a silicon diode (1N4007) with ideality factor (IF) approximately equal to 1.6, as well as on a special silicon diode with an ideality factor equal to unity over many current decades[17,18]

(and therefore practically free from generation-recombination centers) that can be used as a reference. The experimental data have then been compared with results obtained from numerical simulations based on a specifically devised Monte Carlo procedure and on an analytical approach stemming from a modified Shockley-Read-Hall theory (SRH).[19]

The paper is organized as follows: In Sec. II, we present an extension of the Shockley-Read-Hall model[19] for the g-r current, considering different numbers of trap levels in the depletion region; in Sec. III, the connection between charge motion and current is established according to the electrokinematics theorem,[20,21] as well as the approach to compute the power spectral density; in Sec. IV, the Monte Carlo simulation and the measurement results are reported and compared; and in Sec. V, we draw the final conclusions.

II. GENERATION-RECOMBINATION CURRENT AND CARRIER-TRAPPING PROBABILITY

A. Extended SRH model for the generation-recombination current

In Fig. 1, we show the diagram sketching the trap-assisted generation-recombination mechanism. According to standard Shockley-Read-Hall theory,[19] the electron (hole) capture c_N (c_P) and emission e_N (e_P) rate of a trap can be expressed as

$$c_N = c_n n(1-f), \quad c_P = c_p p f, \tag{1}$$

$$e_N = c_n n_i \exp\left(\frac{E_t}{kT}\right) f, \quad e_P = c_p n_i \exp\left(-\frac{E_t}{kT}\right)(1-f), \tag{2}$$

where c_n (c_p) is the electron (hole) capture coefficient, relationships in (2) derive from (1) assuming $c_N = e_N$ and $c_P = e_P$ at the thermodynamic equilibrium, f is the electron occupancy of the trap, and n and p are the electron and hole densities, respectively, which are given by

$$n = n_i \exp\left(\frac{E_{Fn} - E_i}{kT}\right), \tag{3}$$

$$p = n_i \exp\left(\frac{E_i - E_{Fp}}{kT}\right), \tag{4}$$

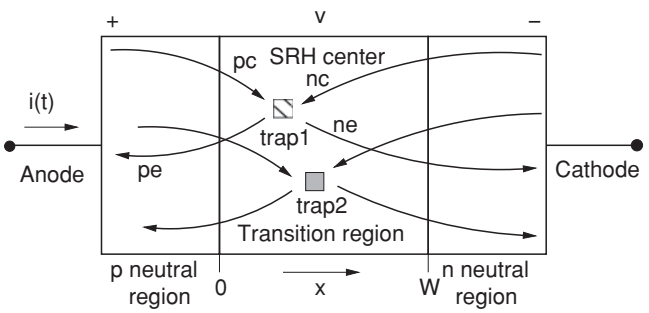

FIG. 1. Sketch of the trap-assisted generation-recombination mechanism in a $p-n$ junction, where trapping and detrapping of electrons and holes in the case of two traps with different energies in the device is also depicted.

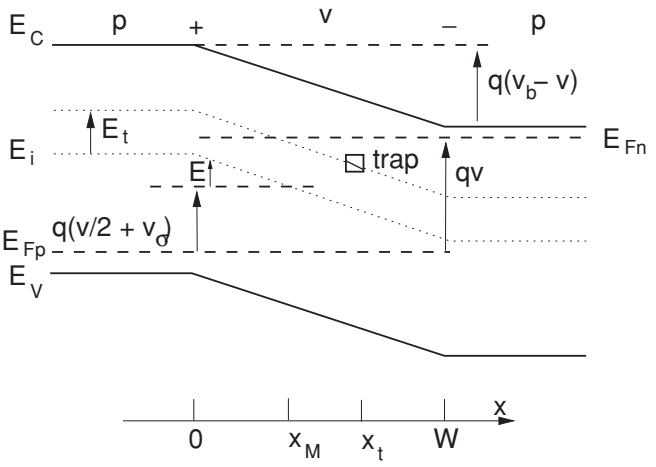

FIG. 2. Schematic energy diagram of a $p-n$ junction.

where n_i ($n_i^2 = np$) is the intrinsic density, E_{Fn}, E_{Fp}, E_{Ft} are the quasi Fermi levels of the electrons (in the n neutral region and into the depletion region), holes (in the p neutral region and into the depletion region), and of the trap, respectively (Fig. 2). The intrinsic Fermi level E_i can be instead expressed as

$$E_i = \frac{E_C + E_V + kT\ln(N_V/N_C)}{2}, \tag{5}$$

where E_C (E_V) is the bottom (top) of the conduction (valence) band and N_C (N_V) is the effective density of states in the conduction (valence) band.

The Fermi-Dirac factor of the trap will then be given by

$$f = \frac{1}{1+\exp\frac{E_t - E_{Ft}}{kT}}, \tag{6}$$

where E_t is the trap energy, measured from E_i. If we now define the rate of trap crossing as

$$u_{rt} \equiv c_N - e_N = c_P - e_P, \tag{7}$$

from (1), (2), (6), and (7), we can express the Fermi-Dirac factor f of the trap as

$$f = \frac{\exp\left(-\frac{v+2v_0}{2V_T}\right) + \exp\left(-\frac{E}{kT}\right)}{2\left[\cosh\left(\frac{E}{kT}\right) + \exp\left(-\frac{v}{2V_T}\right)\cosh\left(\frac{v_0}{V_T}\right)\right]}, \tag{8}$$

where $v = (E_{Fp} - E_{Fn})/q$ is the diode bias voltage (Fig. 2), $V_T = kT/q$ (k and T are the Boltzmann constant and the temperature, respectively), and $qv_0 = E_t + qv_\sigma$ is the effective level of the traps in the depletion region, which accounts for the trap capture coefficient through $v_\sigma = V_T/2\ln(c_n/c_p)$, while (Fig. 2)

$$E = E_i - E_{Fp} - q(v/2 + v_\sigma). \tag{9}$$

From Eqs. (1), (2), (7), and (8), we obtain

$$u_{rt} = u_s \frac{\sinh\left(\frac{v}{2V_T}\right)}{\cosh\left(\frac{E}{kT}\right) + \exp\left(-\frac{v}{2V_T}\right)\cosh\left(\frac{v_0}{V_T}\right)}, \tag{10}$$

where $u_s = \sqrt{c_p c_n} n_i$, with a maximum reached for $E = 0$, i.e., in correspondence of the abscissa x_M (Fig. 2) for which, according to (9),

$$E_i(x_M) = E_{Fp} + q(v/2 + v_\sigma). \tag{11}$$

In the depletion region, the width of which is equal to W_0 for $v = 0$ and, for $v \neq 0$,

$$W = W_0\sqrt{1 - v/v_b}, \tag{12}$$

the electric field can be approximated with a constant value, equal to $-(v_b - v)/W$, where v_b is the built-in voltage $v_b = [E_G - (E_C - E_{Fn}) - (E_{Fp} - E_V)]/q$ and E_G is the energy gap, being the difference $E_C - E_{Fn}$ $(E_{Fp} - E_V)$ considered for $x > W$ $(x < 0)$ (Fig. 2).

Therefore, within the depletion region, we can write $E_i = E_i(0) - q(v_b - v)x/W$, which leads to

$$E = -q\frac{v_b - v}{W}(x - x_M) \tag{13}$$

for $0 < x < W$, while at the boundaries we obtain

$$E(0) = -E_{Fpi} - q(v/2 + v_\sigma) \tag{14}$$

and

$$E(W) = E(0) - q(v_b - v) \tag{15}$$

with $E_{Fpi} = E_{Fp} - E_i(0)$ being the Fermi level in the neutral region p, evaluated with respect to the intrinsic Fermi level $E_i(0)$. In the symmetric case ($n = p$ and $c_n = c_p$), we obtain $E(0) = -E(W) = q(v_b - v)/2$.

Assuming that the traps in the depletion region have a uniform distribution $n_{tj}(\mathbf{r}, v_{0j}) = n_{tj}(v_{0j})$ and an effective energy level equal to qv_{0j}, according to (10) and (13), the total g-r current is computed performing the integral

$$I_r = qA\sum_j n_{tj}(v_{0j})\int_0^W u_{rt}(x, v_{0j})dx = \frac{\sinh\left(\frac{v}{2V_T}\right)}{\sqrt{1 - \frac{v}{v_b}}} \times \sum_j I_{rsj}\int_{\eta_W}^{\eta_0} \frac{1}{\cosh(\eta) + \exp\left(-\frac{v}{2V_T}\right)\cosh\left(\frac{v_{0j}}{V_T}\right)}d\eta, \tag{16}$$

where $\eta = E/kT$, $\eta_0 = E(0)/kT$, $\eta_W = E(W)/kT$, $I_{rsj} = qu_{sj}n_{tj}(V_T/v_b)W_0A$, and A is the diode cross section.

The integral Ψ_j in (16) can be expressed in a closed form (see Appendix A) as

$$\Psi_j = \frac{2}{\sqrt{a_j^2 - 1}}\ln\left(\frac{\sqrt{a_j^2 - 1} - a_j + 1}{\sqrt{a_j^2 - 1} + a_j - 1}\right), \quad a_j > 1 \tag{17}$$

$$\Psi_j = \frac{4}{\sqrt{1 - a_j^2}}\tan^{-1}\sqrt{\frac{1 - a_j}{1 + a_j}}, \quad a_j < 1 \tag{18}$$

which holds for $\eta_0, |\eta_W| > 2$, with $a_j = \exp(-v/2V_T)\cosh(v_{0j}/V_T)$.

For example, for $v_{0j} \approx 60$ mV and $v > 200$ mV, we obtain $a_j = 0.1$ and, from (18), $\Psi_j \approx \pi$, from which the expression for the recombination current $I_r \propto \exp(v/2V_T)/\sqrt{1 - v/v_b}$ of the SRH model is recovered.

The diffusion current can then be expressed as

$$I_d = I_{ds}\left[\exp\left(\frac{v}{V_T}\right) - 1\right] \tag{19}$$

and the total current in the diode becomes

$$I = I_d + I_r, \tag{20}$$

with I_{ds} being the saturation diffusion current.

B. Carrier-trapping probability

A trap containing a hole can change its state in a time interval dt whenever an electron is captured (nc) or a hole is emitted (pe). The probability of an event nc is equal to $dp_{nc} = c_N dt$ and the probability of an event pe is equal to $dp_{pe} = e_P dt$. If we assume that the state changes only once in the interval dt, the relative probability P_{nc} of a electron capture can be expressed as $P_{nc} \equiv dp_{nc}/(dp_{nc} + dp_{pe})$ and finally from (1) and (2), in which, by definition f=0, we obtain

$$P_{nc} = \frac{c_N}{c_N + e_P} = \frac{1}{1 + \exp\left(-\frac{v + 2v_0}{2V_T}\right)\exp\left(\frac{E}{kT}\right)}. \tag{21}$$

Equivalently, the probability P_{pc} of a hole to be trapped, when an electron is already in the trap, can be expressed as

$$P_{pc} = \frac{c_P}{c_N + e_P} = \frac{1}{1 + \exp\left(-\frac{v - 2v_0}{2V_T}\right)\exp\left(-\frac{E}{kT}\right)}, \tag{22}$$

so that $P \equiv P_{nc} + P_{pe} - 1$ reads

$$P = \frac{\sinh\left(\frac{v}{2V_T}\right)}{\cosh\left(\frac{v}{2V_T}\right) + \cosh\left(\frac{qv_0 - E}{kT}\right)}. \tag{23}$$

The above-derived expressions will be used in the following sections in order to compute the current and the noise power spectral density of the g-r mechanism assisted by a trap in the depletion region.

III. INSTANTANEOUS CURRENT AND POWER SPECTRAL DENSITY

A. Instantaneous current

In order to compute the power spectral density of the current fluctuations, the expression for the time-dependent current $i(t)$ is needed. Such a quantity can be determined through the electrokinematics theorem[20,21] (see Appendix B). In particular, for a constant bias v and for frequencies smaller than the inverse of the largest transit time t_{PM} of a carrier traversing the device, $i(t)$ reads

$$i(t) = \sum_{i=1}^{\nu(t)} q_i \mathbf{v}_i \cdot \mathbf{F}(\mathbf{r}_i) = -\sum_{i=1}^{\nu(t)} q_i \frac{d\Phi[\mathbf{r}_i(t)]}{dt}, \tag{24}$$

where q_i, $\mathbf{r}_i$, and $\mathbf{v}_i$ are the charge, position, and velocity of the ith charge in the device, $\nu(t)$ is the number of charges present in the device at the time t, and $\mathbf{F} = -\nabla\Phi$ is an irrotational field, with boundary conditions $\Phi = 1$ and 0 in correspondence of the anode and of the cathode, respectively (see Appendix B). If we consider the carriers only captured and emitted by a single trap, the anode current $i_{rt}(t)$ can be seen as a combination of

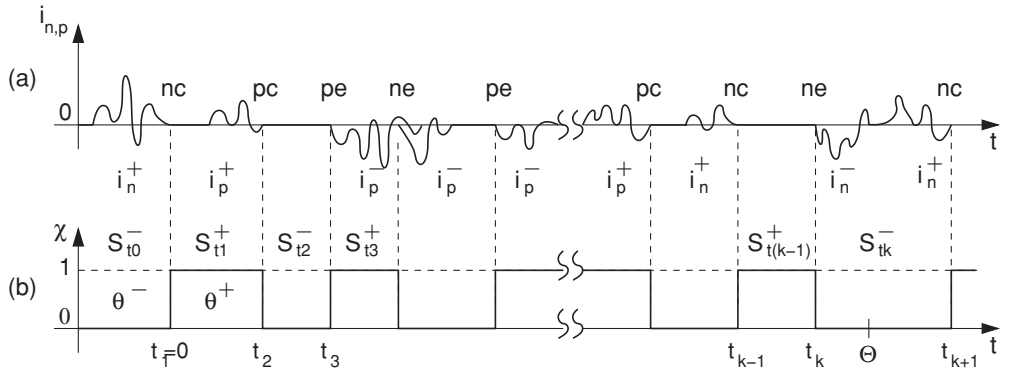

FIG. 3. (a) Current pulses $i_n^{\pm}$ ($i_p^{\pm}$) at the anode associated to electrons (holes) captured (nc,i_n^+) [(pc,i_p^+)] or emitted (ne,i_n^-) [(pe,i_p^-)] from the trap, respectively. (b) Number of electrons ($\chi = 1$ or 0) in a trap as a function of time.

pulses $i_n^{\pm}$ ($i_p^{\pm}$) due to electrons (holes), which are captured (process nc, pulse i_n^+) [(process pc, pulse i_p^+)] or emitted (process ne, pulse i_n^-) [(process pe, pulse i_p^-)] from the trap (Fig. 3).

More in detail, at the end (beginning) of the pulse i_n^+ (i_n^-) [i_p^+ (i_p^-)], when an electron [hole] is trapped (detrapped), we have a change from the trap state S_t^- (S_t^+) [S_t^+ (S_t^-)], with $\chi = 0$ ($\chi = 1$) [$\chi = 1$ ($\chi = 0$)] electrons and lasting θ^- (θ^+) [θ^+ (θ^-)], to the complementary state. Moreover, unlike in Ref. 9, where the simple approximation of distinct square pulses has been assumed in order to derive the expression for the power spectral density, here no assumption is made regarding the shape of the pulses, which can also overlap (Fig. 3).

To compute the mean current and the power spectral density, we need to evaluate the charge

$$Q_{rt} = \int_{-\Theta/2}^{\Theta/2} i_{rt}(t)dt = -\int_{-\Theta/2}^{\Theta/2} \sum_{i=1}^{\nu(t)} q_i \frac{d\Phi[\mathbf{r}_i(t)]}{dt} dt \quad (25)$$

induced at the anode by the pulses within the time interval $(-\Theta/2,\Theta/2)$, which must be wide enough to include a statistically significant number of pulses.

From (25), we obtain

$$N \equiv \frac{Q_{rt}}{q} = \Phi N_{nc} + (1-\Phi)N_{pc} - \Phi N_{ne} - (1-\Phi)N_{pe}, \quad (26)$$

where $\Phi = \Phi(\mathbf{r}_t)$, $\mathbf{r}_t$ is the position of the trap, N_{nc} (N_{pc}) [N_{ne} (N_{pe})] is the number of electrons (hole) trapped [emitted] during the considered time interval.

Let us now show that N is not a function of Φ, i.e., it does not depend on the trap position. Indeed, in a trapping and detrapping cycle, we have the following combinations of possible consecutive events, which determine variations ΔN not depending on Φ: (nc, ne) give $\Delta N_{nc}{=}\Delta N_{ne} = 1$, $\Delta N_{pc} = \Delta N_{pe} = 0$, and from (26), $\Delta N = \Phi - \Phi = 0$; ($nc$, pc), $\Delta N = \Phi + (1-\Phi) = 1$; ($ne$,$nc$), $\Delta N = -\Phi + \Phi = 0$; ($ne$, pe) $\Delta N = -\Phi - (\Phi - 1) = 1$; ($pc$, nc), $\Delta N = (1-\Phi) + \Phi = 1$; ($pc$, pe), $\Delta N = 1 - \Phi - (1-\Phi) = 0$; ($pe$, ne), $\Delta N = -(1-\Phi) - \Phi = -1$; ($pe$, pc), $\Delta N = -(1-\Phi) + (1-\Phi) = 0$.

For simplicity, we can assume $\Phi = 1 - \Phi$, i.e., $\Phi = 1/2$, which gives

$$N = \tfrac{1}{2}(N_{nc} + N_{pc} - N_{ne} - N_{pe}). \quad (27)$$

Defining $\theta_n = \langle\theta^+\rangle$, $\theta_p = \langle\theta^-\rangle$, and $m = \Theta/(\theta_n + \theta_p)$, the mean number of cycles within the Θ interval, we obtain $\langle N_{nc}\rangle = mP_{nc}$, $\langle N_{pe}\rangle = m(1-P_{nc})$, $\langle N_{pc}\rangle = mP_{pc}$, and $\langle N_{ne}\rangle = m(1-P_{pc})$, so that the mean current through the trap reads

$$\overline{i_{rt}} = \frac{Q_{rt}}{\Theta} = qu_{rt}, \quad (28)$$

and, through (27), one gets

$$u_{rt} = \frac{P}{\theta_n + \theta_p}, \quad (29)$$

where $P = P_{nc} + P_{pc} - 1$ given by (23) can be seen as the efficiency of the trap in conducting the current.

B. Mean trapping and detrapping times

The mean times θ_n and θ_p of an electron and a hole being trapped can be obtained from (29) and from the trap occupation factor f of an electron written as

$$f = \frac{\theta_n}{\theta_n + \theta_p}, \quad (30)$$

which, together with (8), (10), (23), and (29), gives

$$\theta_p = \frac{\exp\left(\frac{2v_0 - v}{2V_T}\right) + \exp\left(\frac{E}{kT}\right)}{2u_s\left[\cosh\left(\frac{qv_0 - E}{kT}\right) + \cosh\left(\frac{v}{2V_T}\right)\right]}, \quad (31)$$

$$\theta_n = \frac{\exp\left(-\frac{v+2v_0}{2V_T}\right) + \exp\left(-\frac{E}{kT}\right)}{2u_s\left[\cosh\left(\frac{qv_0 - E}{kT}\right) + \cosh\left(\frac{v}{2V_T}\right)\right]}. \quad (32)$$

C. Power spectral density

From Milatz's theorem,[22] the power spectral density S_{rt} of the current $i_{rt}(t)$ through a trap, at frequencies smaller than

$1/t_{PM}$, reads

$$S_{rt} = \lim_{\Theta\to\infty}\frac{2}{\Theta}\left\langle\left[\int_{-\Theta/2}^{\Theta/2}\Delta i_{rt}dt\right]^2\right\rangle \approx \frac{2}{\Theta}\mathrm{var}(Q_{tr}) = \frac{2q^2}{\Theta}\mathrm{var}(N), \tag{33}$$

where $\Delta i_{rt} = i_{rt} - \overline{i_{rt}}$ is the current fluctuation, the third term [deriving from (25)] holds for $\Theta \gg t_{PM}$, while the fourth term follows from (26).

From (26), (28), and (33), we also obtain

$$S_{rt} = 2q(qu_{rt})\varphi_{rt}, \tag{34}$$

where

$$\varphi_{rt} \equiv \frac{\mathrm{var}(N)}{\langle N\rangle}. \tag{35}$$

If the traps are sufficiently far from each other, their fluctuations can be considered statistically independent and the total power spectral density S_r, from (34), can be expressed as

$$S_r = A\sum_j n_{tj}\int_0^W S_{rtj}dx = 2q^2A\sum_j n_{tj}\int_0^W u_{rtj}\varphi_{rtj}dx, \tag{36}$$

which, exploiting (10) and (16), becomes

$$S_r = 2q\frac{\sinh\left(\frac{v}{2V_T}\right)}{\sqrt{1-\frac{v}{v_b}}}\sum_j I_{rsj} \times\int_{\eta_W}^{\eta_0}\frac{\varphi_{rtj}}{\cosh(\eta)+\exp\left(-\frac{v}{2V_T}\right)\cosh\left(\frac{v_{0j}}{V_T}\right)}d\eta. \tag{37}$$

From (19) and exploiting Schottky's theorem,[1] the power spectral density of the full shot noise associated to the diffusion current I_d can be expressed as

$$S_d = 2qI_{ds}\left[\exp\left(\frac{qv}{V_T}\right)+1\right] = 2qI_d\coth\left(\frac{v}{2V_T}\right), \tag{38}$$

while the full shot noise S_{rsh} associated to I_r [given by (16)] in the absence of any generation-recombination events reads

$$S_{rsh} = 2qI_r\coth\left(\frac{v}{2V_T}\right). \tag{39}$$

We can now define the total Fano factor $F \equiv (S_d+S_r)/(S_d+S_{rsh})$ as the ratio between the measured noise power spectrum (S_d+S_r) and the full shot noise power spectrum (S_d+S_{rsh}), which, from (16), (37), (38), and (39), finally reads

$$F = \frac{I_d}{I}F_d + \frac{I_r}{I}F_r, \tag{40}$$

where $F_d = 1$ and

$$F_r = \frac{\sum_j I_{rsj}\int_{\eta_W}^{\eta_0}\frac{\varphi_{rtj}}{\cosh(\eta)+\exp\left(-\frac{v}{2V_T}\right)\cosh\left(\frac{v_{0j}}{V_T}\right)}d\eta}{\sum_j I_{rsj}\int_{\eta_W}^{\eta_0}\frac{1}{\cosh(\eta)+\exp\left(-\frac{v}{2V_T}\right)\cosh\left(\frac{v_{0j}}{V_T}\right)}d\eta}\tanh\left(\frac{v}{2V_T}\right) \tag{41}$$

are the Fano factors of the diffusion and the g-r current, respectively.

IV. MONTE CARLO SIMULATIONS AND MEASUREMENT RESULTS

In this section, we first introduce the numerical approach adopted to compute the I-V characteristics and the Fano factor, which will be then compared with experimental data obtained for three different diodes. The purposely devised method is based on Monte Carlo simulations of the generation-recombination process, where traps are considered independent, as assumed in Ref. 9. We want to point out anyway the fact that our method is general and can be easily extended to the case of interacting traps.

A. Simulation method

Let us assume an exponential distribution $M(\rho)$:

$$M = \frac{1}{\sigma}\exp\left(-\frac{\rho}{\sigma}\right) \tag{42}$$

for the trapping and detrapping random time variable ρ, being $\rho = \theta^+$ $(\rho = \theta^-)$ and $\sigma = \theta_n$ $(\sigma = \theta_p)$ for the state S_t^+ (S_t^-) (Fig. 3). Since the states S_t^+ (S_t^-) corresponding to a trapped electron (hole) have the same probability, we can write $M = b/\sigma$, where b is a random variable uniformly distributed in the interval $(0,1)$, and the state S_t^+ (S_t^-) lasts a time ρ,

$$\rho = -\sigma\ln b. \tag{43}$$

As a consequence, if we define $\tau = \rho u_s$ as the dimensionless time that a charge remains trapped, we can express the trapping and detrapping times τ^+ and τ^-, respectively, as

$$\tau^+ = -u_s\theta_n\ln b, \tag{44}$$

$$\tau^- = -u_s\theta_p\ln b, \tag{45}$$

where, in accordance to (31) and (32), $u_s\theta_n$ $(u_s\theta_p)$ depends on the trap energy qv_0, extracted via a numerical fitting of the experimentally measured current, and does not depend on the (unknown) carrier capture coefficients.

To compute $\langle N\rangle$ and $\mathrm{var}(N)$, we need to consider a large enough number of events (i.e., changes in the trap state) to obtain reliable statistics. Such a requirement is, for example, satisfied considering $\Theta \gg (\theta_n+\theta_p)$ or, equivalently, $u_s\Theta \equiv \Theta' = u_s(\theta_n+\theta_p)l$, where l must be larger than several thousands.

Before the initial time step $t_1' = u_st_1 = 0$ [Fig. 3(b)], with $t' \equiv u_st$ the dimensionless time, the trap can be either full or empty of an electron (trap in the S_{t0}^+ and S_{t0}^- state, respectively). If the initial state is S_{t0}^-, as shown in Fig. 3(b), at $t_1' = 0$ we can have two possible events $nc = \alpha_1\beta_1$ or $pe = \alpha_1\beta_1$, which leads to the state S_{t1}^+ by indicating with $\alpha = n$ or $\alpha = p$ the carrier type and with $\beta = c$ or $\beta = e$ the trapping and detrapping type. The two events are chosen depending on the value that a random variable γ, uniformly distributed between 0 and 1, assumes: if $0 \leqslant \gamma \leqslant P_{nc}$, we have to choose $\alpha_1\beta_1 = nc$, and we decide for $\alpha_1\beta_1 = pe$ otherwise, with $\Delta N_{\alpha_1\beta_1} = 1$ and $\Delta N_{\alpha_1'\beta_1'} = 0$ for $\alpha_1' \neq \alpha_1$ and $\beta_1' \neq \beta_1$.

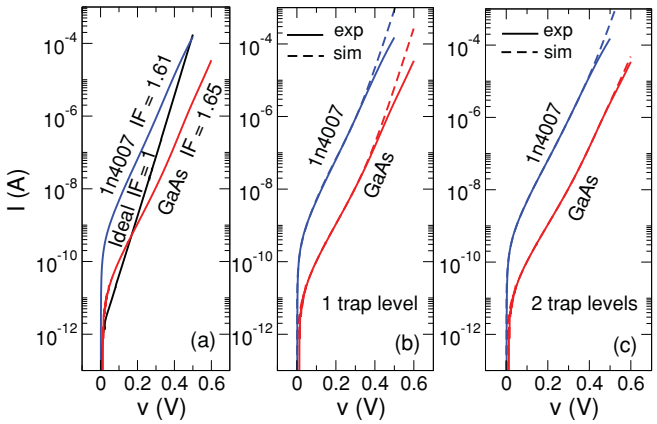

FIG. 4. (Color online) (a) Experimental current-voltage characteristics of Si quasi-ideal, Si 1N4007, and GaAs diodes; Experimental and simulated characteristics of the GaAs and 1N4007 diodes, considering (b) 1 trap level and (c) 2 trap levels.

The state S_{t1}^{+} lasts up to $t_2' = t_1' + \tau_1^{+}$, where τ_1^{+} is obtained from (44). At t_2', the state S_{t2}^{-} starts with an event $\alpha_2\beta_2 = pc$ if another random variable δ satisfies $0 \leqslant \delta \leqslant P_{pc}$, otherwise, $\alpha_2\beta_2 = ne$, with increments $\Delta N_{\alpha_2\beta_2}$ similar to those found for the state S_{t1}^{+}. State S_{t2}^{-} lasts up to $t_3' = t_2' + \tau_2^{-}$, where τ_2^{-} is obtained from (45). The simulated history ends after k steps, when $t_k' \leqslant \Theta'$ and $t_{k+1}' > \Theta'$, obtaining, through the increments $\Delta N_{\alpha\beta}$ and (27), the value for N.

The simulation is performed for many histories to obtain reliable estimates for $\langle N \rangle$ and var(N). This procedure is repeated as a function of the trap position, with a resolution sufficient to compute the integral in (41) with good precision, and for each of the energy levels that have to be included to achieve the best fit between the experimental and theoretical current values given by (16).

In the case of independent traps, such as the one we are studying, the power spectral density for a single trap, given by the following equation (46), has a value corresponding to the results in Ref. 9.

B. Experimental and numerical results

In Fig. 4(a), we show the experimental characteristics of a silicon quasi-ideal diode (almost without traps, thanks to a specific gettering procedure[17,18]) of a GaAs diode for temperature measurements, and of a silicon diode 1N4007, as well as the numerical fits of the I-V characteristic obtained using one [Fig. 4(b)] or two trap levels [Fig. 4(c)] by directly exploiting (16). The obtained fitting parameters are shown in Table I. As can be seen, inclusion of two trap levels leads to a better fit of the current.

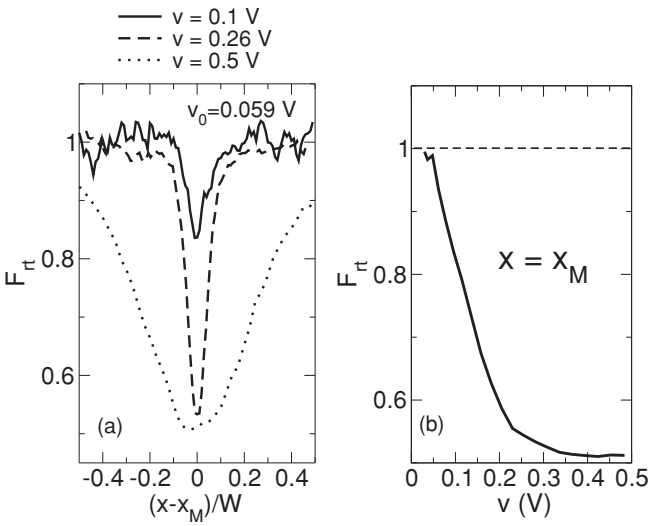

FIG. 5. Fano factor of a trap for the GaAs diode, computed as a function (a) of the trap position x for different bias values v and (b) of v at $x = x_M$.

To investigate the effects of the generation-recombination process on noise when a single trap is considered, we can define its Fano factor $F_{rt} \equiv \frac{S_{rt}}{S_{rtsh}}$ that, according to (34) and (39), i.e., with $S_{rtsh} = 2q(qu_{rt})\coth(v/2V_T)$, becomes

$$F_{rt} = \frac{S_{rt}}{2q(qu_{rt})\coth(v/2V_T)} = \varphi_{rt}(x,v)\tanh\left(\frac{v}{2V_T}\right), \qquad (46)$$

which, for instance, in the case of GaAs and of a single level (with $q v_0 = 0.059$ eV and v_b=0.7 V), yields the results shown in Fig. 5. As can be seen, the g-r processes determine a reduction of the power spectral density with respect to the full shot value down to 1/2 for large v and in correspondence of x_M, while, for low v or at the boundaries of the depletion region, $F_{rt} \to 1$.

The result $F = 1$ for the quasi-ideal diode follows from the same considerations. There is a simple intuitive explanation for the computed V-shape behavior, shown in Fig. 5: For low values of the current, i.e., for low voltage or far from x_M, the occupancy (or vacancy) of the the trap is much lower than 1 [see (8)], therefore, almost no correlation is introduced between electrons (holes) crossing the device [since the probability that one electron (hole) will be delayed as a result of the trap being full (empty) is negligible]; as the current increases, also the trap occupancy (or vacancy) increases

TABLE I. Current fitting parameter, considering one and two trap levels. qv_{01} and qv_{02} are the trap levels; I_m and I_M are the lower and upper bounds of the current interval within which the fitting has been performed; I_{ds} is the diffusion saturation current; and I_{rs1} and I_{rs2} are the saturation currents of the g-r component, considering one and two trap levels, respectively.

Diode	qv_{01} (eV)	qv_{02} (eV)	I_m (A)	I_M (A)	I_{ds} (A)	I_{rs1} (A)	I_{rs2} (A)
Si	0.077		10^{-10}	2×10^{-6}	3.32×10^{-12}	7.67×10^{-10}	
Si	0.065	0.18	3×10^{-11}	1×10^{-5}	1.31×10^{-12}	5.77×10^{-10}	9.19×10^{-10}
GaAs	0.059		10^{-11}	3×10^{-8}	2.25×10^{-14}	1.25×10^{-11}	
GaAs	0.056	0.265	2×10^{-11}	2×10^{-6}	2.31×10^{-15}	1.21×10^{-11}	5.11×10^{-11}

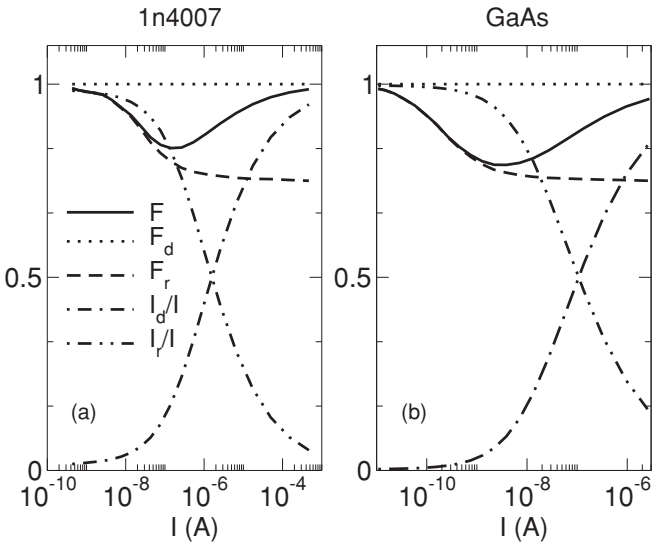

FIG. 6. Ratio I_r/I (I_d/I) between the g-r current I_r (diffusion current I_d) and the total current I and their simulated Fano factors F_r, F_d, and F, respectively, for the (a) 1N4007 and (b) GaAs diodes, considering one trap level.

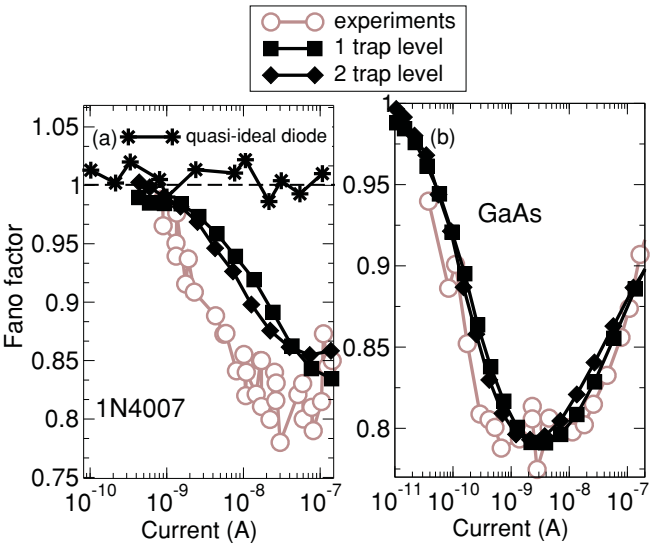

FIG. 7. (Color online) Experimental (circles) and simulated Fano factors considering one trap level (squares) and two trap levels (diamonds) for (a) the 1N4007 diode and (b) the GaAs diode. In (a), the experimental Fano factor (stars) of a quasi-ideal diode is also shown.

($f \to 1/2$), leading to correlations and to a suppression of shot noise in the current component flowing through the trap.

In Fig. 6, we show the computed ratio I_r/I (I_d/I) between the g-r current I_r (diffusion current I_d) and the total currents I and their simulated Fano factor F_r, F_d, and F, respectively, for the 1N4007 and GaAs diodes. Such a picture highlights the contribution of the different components (both g-r and diffusion) to the total Fano factor F. Also, F has a V-shape behavior (found also in measurement results) as a function of the current, and this can be explained by the fact that, at low currents, both F_d and F_r [according to (41), (46), and Fig. 5] are equal to 1, whereas, at high currents, where the g-r Fano factor $F_r \to 3/4$,[9] its current fraction I_r/I tends to zero, and, again, $F_d \to 1$.

Noise measurements on the three types of $p-n$ junctions can be performed using a cross-correlation technique[23] based on two amplifiers that are connected in a "series" or "parallel" configuration depending on the differential impedance of the diode. At lower bias currents, the differential impedance is high, thus, the prevailing noise contribution from the amplifier is represented by the equivalent input noise current generator, the effect of which can be minimized with the series configuration, which we have used in our measurements. Moreover, a particular procedure has been applied to precisely evaluate the amplifier transimpedance, as detailed in Ref. 24. In Fig. 7, we show the comparison between the experimental and the numerical Fano factor for the quasi-ideal and 1N4007 silicon diodes [Fig. 7(a)] as well as for the GaAs diode [Fig. 7(b)], considering one and two trap levels.

We observe that the two-level trap model allows a better fit of the diode characteristic (although the single-level model already provides good results) (Fig. 4) as well as of the Fano factor (Fig. 7) for the 1N4007 diode, while the single-level model provides better results for the noise of the GaAs diode. The single-level model also allows faster calculations, due to the reduced computational complexity.

V. CONCLUSION

In this paper, we have investigated shot noise suppression in $p-n$ junctions due to generation-recombination phenomena. We have obtained expressions for the Fano factor in such devices and we have performed a numerical Monte Carlo evaluation of its parameters. We have also performed measurements of the Fano factor over a wide current range (from 10^{-11} A to 2×10^{-7} A) on three different $p-n$ junctions using a very sensitive system based on the cross-correlation technique, obtaining results that represent a significant improvement over what was available in the literature. In particular, it has been possible to experimentally observe the decrease, with increasing current, of the Fano factor (down to 0.8) associated with the rising occupancy of the trap and its increase back to unity, at higher current values, due to the prevalence of the diffusion current, which is characterized by the unitary Fano factor. As a verification, we have measured also the Fano factor for a quasi-ideal diode, in which generation-recombination phenomena are negligible, finding the expected full shot noise over a wide current range.

These experimental results have been interpreted by means of an analytical model and an associated numerical simulation. The model is based on an extended expression of the SRH current and on the electrokinematics theorem for the evaluation of current fluctuations. Starting from the average rate of charges crossing the device via a trap in the depletion region, we have obtained an expression for the stationary current, which we have used to determine the mean trapping and detrapping times and the capture probability of a charge in the trap. Such quantities and the trap energy levels obtained by fitting the experimentally measured and the theoretical I-V characteristics have then been included into a numerical Monte Carlo simulation in order to compute the power spectrum of the g-r noise component and the overall Fano factor. Comparison with the experimental data has shown that I-V characteristics

are best fitted by means of a two-level model, which has also provided a good representation of the V-shape behavior of the Fano factor as a function of the bias current.

APPENDIX A

The integral

$$\Psi_j = \int_{\eta_W}^{\eta_0} \frac{d\eta}{a_j + \cosh(\eta)} \tag{A1}$$

can be expressed as

$$\Psi_j = \frac{1}{\sqrt{a_j^2 - 1}} \ln\left(\frac{\sqrt{a_j+1} - \sqrt{a_j-1}\tanh(\eta/2)}{\sqrt{a_j+1} + \sqrt{a_j-1}\tanh(\eta/2)} \right)\Bigg|_{\eta_W}^{\eta_0}, \quad a_j > 1 \tag{A2}$$

$$\Psi_j = \frac{2}{\sqrt{1-a_j^2}} \tan^{-1}\left(\sqrt{\frac{1-a_j}{1+a_j}} \tanh(\eta/2) \right)\Bigg|_{\eta_W}^{\eta_0}, \quad a_j < 1. \tag{A3}$$

In the symmetric case, $\eta_0 = -\eta_W = (v_b - v)/2V_T$. If $v_b = 0.7$ V and $v = v_{\max} = 0.4$ V, which is the maximum value in our case, we obtain $\eta_0/2 = 3$ and $\tanh(\eta_0/2) \approx 1$ for $v < 0.4$ V, so that (A2) and (A3) reduce to (17) and (18), respectively.

APPENDIX B

According to the electrokinematics theorem,[20,21] the current flowing into the anode of the device is given by

$$i(t) = \sum_{i=1}^{\nu(t)} \left[q_i \mathbf{v}_i \cdot \mathbf{F}(\mathbf{r}_i) + \frac{de_i}{dt} \right] + C\frac{dv}{dt}, \tag{B1}$$

where C is diode capacitance, and q_i, $\mathbf{r}_i$, and $\mathbf{v}_i$ are the charge, position, and velocity of the ith charge of the $\nu(t)$ charges that are present in the device at time t. $\mathbf{F} = -\nabla\Phi$ is an irrotational field, which satisfies $\nabla \cdot (\varepsilon \mathbf{F}) = 0$ (where ε is the dielectric constant) with boundary conditions $\Phi = 1$ and 0 at the anode and at the cathode, respectively, and appropriate boundary conditions on the ungated surface S_R of the device. de_i/dt accounts for the displacement current through S_R, due to the motion of the ith charge, and e_i becomes equal to zero when such a charge enters an electrode, so that its contribution in terms of Fourier transform, necessary to compute the noise spectrum, becomes negligible for frequencies smaller than $1/t_{PM}$.

As a consequence, for such frequencies and for a constant bias v, we obtain (24), and for a cylindrical device with length equal to L, and $\mathbf{F}$ along the x axis of the device, i.e., $\mathbf{F} = F_x\mathbf{i} = \mathbf{i}/L$, (B1) reduces to the well-known Ramo-Shockley theorem[25]

$$i(t) = \sum_{i=1}^{\nu(t)} q_i \frac{v_{xi}}{L} + C\frac{dv}{dt}. \tag{B2}$$

[1] W. Schottky, Ann. Phys. (Leipzig) **57**, 541 (1918).
[2] Ya. M. Blanter and M. Büttiker, Phys. Rep. **336**, 1 (2000).
[3] Y. P. Li, A. Zaslavsky, D. C. Tsui, M. Santos, and M. Shayegan, Phys. Rev. B **41**, 8388 (1990).
[4] L. Y. Chen and C. S. Ting, Phys. Rev. B **43**, 4534 (1991).
[5] H. C. Liu, J. Li, G. C. Aers, C. R. Leavens, M. Buchanan, and Z. R. Wasilewski, Phys. Rev. B **51**, 5116 (1995).
[6] I. A. Maione, M. Macucci, G. Iannaccone, G. Basso, B. Pellegrini, M. Lazzarino, L. Sorba, and F. Beltram, Phys. Rev. B **75**, 125327 (2007).
[7] Ya. M. Blanter and M. Büttiker, Phys. Rev. B **59**, 10217 (1999).
[8] G. Iannaccone, G. Lombardi, M. Macucci, and B. Pellegrini, Phys. Rev. Lett. **80**, 1054 (1998).
[9] P. O. Lauritzen, IEEE Trans. Electron Devices **15**, 770 (1968).
[10] K. M. Van Vliet, IEEE Trans. Electron Devices **32**, 1236 (1976).
[11] J. A. Jimenez Tejada, A. Godoy, A. Palma, and P. Cartujo, J. Appl. Phys. **90**, 3998 (2001).
[12] B. Schneider and M. J. O. Strutt, Proc. IRE **47**, 546 (1959).
[13] T. E. Wade and A. Van Der Ziel, Solid-State Electron. **19**, 909 (1976).
[14] G. Blasquez, Solid-State Electron. **21**, 1425 (1978).
[15] Y. Dai and H. Chen, Solid-State Electron. **34**, 259 (1991).
[16] I. A. Maione, G. Fiori, L. Guidi, G. Basso, M. Macucci, B. Pellegrini, *Proc. Int. Conf. on Noise and Fluctuations, ICNF 2009 (Pisa, Italy, 2009)*, edited by G. Basso and M. Macucci (AIP Conference Proceedings), p. 221.
[17] G. F. Cerofolini and M. L. Polignano, J. Appl. Phys. **55**, 579 (1984).
[18] B. Pellegrini, J. Appl. Phys. **71**, 5504 (1992).
[19] W. Shockley and W. T. Read, Phys. Rev. **87**, 835 (1952); R. N. Hall, *ibid.* **87**, 387 (1952).
[20] B. Pellegrini, Phys. Rev. B **34**, 5921 (1986).
[21] B. Pellegrini, Nuovo Cimento D **15**, 855 (1993).
[22] A. van der Ziel, *Noise in Solid State Device and Circuits* (Wiley, New York, 1986), p. 16.
[23] L. Fasoli, M. Sampietro, and G. Ferrari, Rev. Sci. Instrum. **70**, 2520 (1999).
[24] B. Pellegrini, M. Macucci, and G. Basso, in *Advanced Experimental Methods for Noise Research in Nanoscale Electronic Devices*, edited by J. Sikula and M. Levinshtein (Kluwer Academic, Dordrecht, 2004), p. 203.
[25] S. Ramo, Proc. IRE. **27**, 584, (1939); W. Shockley, J. Appl. Phys. **9**, 635 (1938).